Electronic Supplementary Material (ESI) for Sustainable Energy & Fuels.

Supplementary information for: Closing the balance - on the role of integrating biorefineries in the future energy system

Julia Granacher[1*], Rafael Castro-Amoedo[1], Jonas Schnidrig[1], François Maréchal[1]

10th July 2023

[1]Industrial Process and Energy Systems Engineering group, École Polytechnique Fédérale de Lausanne, Rue de l'Indutrie 17, 1950 Sion, Switzerland;
*julia.granacher@epfl.ch

Contents

A Supplementary information on the superstructure model

In the following, supplementary material on the characteristics of the superstructure is provided. Detailed descriptions of the considered superstructure for combined pulp and fuel production, including the Kraft pulp mill, thermochemical conversion pathways and fuel synthesis models are available in [1], the following provides a summary of the process model parameters.

Table 1: Kraft pulp mill.

	Unit	**Value**	**References**
Pulp mill			
Pulp production	adt/day	1000	[2]
Black liquor stream	kg/s for 1000 adt pulp/day	14.89	[2]
Bark stream	kW bark/adt pulp	33.5	[3]
Lime kiln and chemical recovery			[4, 5]
$T^{calcination}$	°C	900	[4, 5]
$T^{product}$	°C	300	[6]
Reburn specific heat	J/kg/K	989	[4]
CO_2 specific heat	J/kg/K	919	[4]
Heat of calcination	kJ/kg	3270	[4]
Inerts specific heat	J/kg/K	1046	[4]
Availability	%	85	[6]
Dust loss	%	5	private data
Solid content	%	73.5	private data
Enthalpy of evaporation	kJ/kg	2439	[4]
Na_2CO_3 in smelt	g/kg dry solids black liquor	278.3	[7]
Shell losses in kiln	% of heat input	15	[8]

A.1 Thermoechmical conversion pathways

Table 2: Black liquor gasification.

	Unit	Value	References
Gasification of black liquor			
Hydrolysis			[9]
Lignin fraction in organic biomass	wt $\%_{DAF}$	94	
H/C-ratio of lignin	mol_{DAF}	1.11	
O/C-ratio of lignin	mol_{DAF}	0.33	
Effective water content	wt%	93	
Decomposition of carboxylic salts			[10],[11]
Reactor yield	-	0.7	
Salt separator			[12]
Recovery of inorganic cooking chemicals	%	100	[13]
Organic losses in salt brine	%	10	[9]
Hydrothermal Gasification			[9]
Reactor temperature	°C	700	[14]
Reactor pressure	bar	250	[15]
Gas expander isentr. efficiency	–	0.8	[15]
Liquid expander isentr. efficiency	–	0.82	[15]
Pressure Swing adsorption (PSA)			[16]
Recovery	%	52	
Purity	mol%	99.996	
Number of beds	-	4	
Operating pressure	bar	30	[17]
Operating temperature	°C	25	[18]
Adsorbent		Activated carbon/zeolite	
Selexol and Pressure Swing adsorption			[9, 17, 19]
Pressure selexol/ PSA	bar	70/ 30	
Temperature selexol/ PSA	°C	25	
Recovery H_2 selexol	%	100	
Recovery H_2 PSA	%	80	
Number of beds PSA	-	6	
Purity	mol %	99.997	
COS hydrolysis			[20]
Temperature	°C	220	

Pressure	bar	depending on AGR unit	
Warm-Temperature Syngas Desulfurization			[21, 22]
Temperature	°C	330	
Pressure	bar	30	

Table 3: Termochemical conversion pathways of bark.

	Unit	Value	References
Pretreatment			[23–26]
Drying technology	-	Steam/air drying	
Moisture content after drying	%	10 (FT) / 20	
Gasification			[23–26]
Operating conditions (T,p), agent, steam to dry biomass ratio			
Directly heated entrained flow (ENF)	°C, bar, -,-	1350, 30, oxygen-steam, 0.6	
Directly heated circulating fluidized bed (CFB)	°C, bar, -,-	850,1, oxygen-steam, 0.6	
Indirectly heated fast internally circulating fluidized bed (FICFB)	°C, bar, -,-	850,1, oxygen-steam, 0.5	
Gas conditioning			[23–26]
Gas cleaning technology	-	cold/hot	
Gas cleaning temperature	°C	150 / 850	
Gas cleaning filter pressure drop	mbar	1000	
Gas cleaning flash temperature	°C	25	
water gas shift (WGS) temperature	°C	300	
CO_2 removal	-	MEA	[27]
MEA heat requirements	MJ/kg CO_2	3.3 (at 150°C, 20% recoverable)	
MEA electricity requirements	kJ/kg CO_2	25	
Fuel synthesis			[23–26]
Operating conditions			
Fischer-Tropsch (FT) synthesis pressure, temperature	bar, °C	25,220	
dimethyl ether (DME) synthesis pressure, temperature	bar, °C	50,277	
methanol synthesis pressure, temperature	bar, °C	85,315	
synthetic natural gas (SNG) synthesis pressure, temperature	bar, °C	5,327	
Technology and catalyst			

FT synthesis	Multi tubular fixed bed reactor, $Co/Zr/SiO_2$	
DME synthesis	Slurry phase reactor , ACZ, HZSM-5	
Methanol synthesis	Multi-stage fixed bed reactor , Cu/ZnO/Al2O3	
SNG synthesis	Internally cooled fluidized bed reactor , NiAl2O3	
Upgrading		[23–26]
FT upgrading	Private data	
DME upgrading	Flash distillation	
Methanol upgrading	Flash distillation	
SNG upgrading	Membranes, PSA	
Fuel specifications		[23–26]
FT specification, temperature, pressure	-, °C , bar	Liquid fuels, 25, 1
DME specification, temperature, pressure	-, °C , bar	99.8 vol%, 25, 1
Methanol specification, temperature, pressure	-, °C , bar	99.4 vol%, 25, 1
SNG specification, temperature, pressure	-, °C , bar	96 vol%, 25, 50

A.2 Fuel cell and co-electrolysis

Table 4 summarizes the key modeling assumptions for the electrolysis and fuel cell models added to the superstructure.

A.3 Carbon capture, mineralization, and geological sequestration

The models for direct and indirect mineralization are adapted from Ostovari, Sternberg and Bardow [31] and Spínola et al. [32], considering serpentine as possible feedstock to complement residues from the mill. Hereafter, the main process modeling assumptions are summarized; details on the adapted simulation models can be found in [33].

Table 4: SOEC/SOFC units.

	Unit	Value	Reference
Alkaline electrolysis			
Water in	kg/s	0.080	[28]
Hydrogen out	kg/s	0.069	[28]
Oxygen out	kg/h	0.170	[28]
Electricity in	kWh	1000	[28]
System efficiency	kWe/kg H_2	52	[28]
Solide oxide Co-electroysis			[29]
Water inlet	kg/s	1.533	
CO_2 input	kg/s	2.64	
Syngas produced	kg/s	3.011	
Oxygen co-produced	kg/s	1.162	
Electricity input	kW	18336	
Solide oxide fuel cell			[30]
F^{min}	kWe	250	
CH_4 in	kg/s	1	
CO_2 out	kg/s	2.75	
η^{elec}	%	75	

Table 5: Direct mineralization.

	Unit	Value	Reference
Grinding and magnetic separation			[31, 34]
Serpentine in	t	2.3	
Electricity demand	kWh	190	
Magnetic material out	t	0.2	
Carbonation reactor and postprocessing			[31, 34]
Operating temperature	°C	155	
Operating pressure	bar	140	
$MgCO_3$ out	t	1.9	
SiO_2 out	t	0.9	
Solvent recovery rate	%	90	

Table 6: Indirect mineralization.

	Unit	Value	Reference
Grinding and Phase 1 reactor: mineral extraction			[31, 34]
Serpentine in	t	3.9	
Electricity demand	kWh	63	
Ammonium sulfate makeup	t	0.3	
Phase 2 reactor: hydroxide formation			[31, 34]
Operating temperature	°C	50	
Operating pressure	bar	0.5	
Phase 3 reactor: carbonation and postprocessing			[31, 34]
Operating temperature	°C	300	
Operating pressure	bar	25	
$MgCO_3$ out	t	2	

Carbon capture is modeled as a blackbox model of monoethanolamine (MEA) with specific heat and electricity requirements and performance indicators from Heyne and Harvey [27]. For geological sequestration, compression of CO_2 to high-pressure levels for transportation is required. The costs for transport and storage are provided in Table 14. Sequestration and MEA modeling assumptions are summarized in Table 7.

Table 7: Carbon capture and sequestration.

	Unit	Value	Reference
CO_2 capture technology			[27]
Electricity demand	kJ/kg CO_2	25	
Heat demand, temperature	MJ/kg CO_2, °C	3.3, 150[a]	
CO_2/water removal rate	%	95	
Sequestration			
Pressure	bar	60	[35]

[a] 20% of heat are recoverable between 90 and 40°C [27].

A.4 Residential district

Table 8 provides information about the heating technology units and the photovoltaic units. The investment costs for the installation of the district heating network (DHN) are calculated using the approach provided in [36] with specific cost data from Belfiore [37], and average heat loss assumptions from Masatin, Latõšev and Volkova [38]. Two types of district heating networks are considered in the superstructure, a fourth generation, medium-temperature water district heating network, operating at supply and return temperatures of 60 °C and 30 °C, respectively, as well as an innovative fifth-generation district heating network, operating on CO_2 as the working fluid with supply and return temperatures of 15 °C and 13 °C. Both DHN models are adapted from RA Suciu [36].

For providing the heat at the required temperature levels for space heating and domestic hot water demands, heat pumps can be installed at the district level; the models are adapted from RA Suciu [36] and Henchoz et al. [39]. The network is balanced using a central plant that exchanges heat with the pulp mill and can provide additional heat to the DHN by heat pumping (CO_2 network, heat pump model adapted from RA Suciu [36]) or a conventional boiler operation (water network, boiler model adapted from [40]). The residential district model is limited by simplifications regarding temperatures of the demands and their dependency on external conditions. For modeling transportation efficiencies, the assumption in Table 9 are used. Table 10 provides the energy content of the fuels used for the analysis of the transportation demands, further elaborated the main article.

Table 8: District model characteristics.

	Unit	Value	Reference
District heating network			[30, 39, 41]
Water network, T^{supply}, T^{return}	°C	60, 30	
CO_2 network T^{supply}, T^{return}	°C	15, 13	
CO_2 network pressure	bar	50	
Conventional heating system			
Fuel split in commune heating	%	20/40/40 (gas/oil/other)	[42]
Efficiency gas boiler	%	95	[43]
Photovoltaic			[36, 44]
T^{a}	°C	15	
T^{ref}	°C	25	
U^{glass}	W/m^2	29.1	
Solar irradiation through PV glass f^{glass}	-	0.9	
Efficiency $\eta^{\text{pv,ref}}$	-	0.14	
$\eta^{\text{pv,variation}}$	-	0.001	
Electricity provision^a, $E^{-,\text{pv}}$	kW	1.66	

^{a}for reference area of A=100 m^2 and irradiation I=100 W/m^2.

Table 9: Efficiency of transport mediums.

Modelling assumptions	**Unit**	**Value**	**Reference**
in 2019			[45]
Fuel-powered car	MJ/pkm	1.78	
Electric car	kWh/vkm	0.17	[46]
Bus	MJ/pkm	1.01	
Freight	MJ/tkm	2.74	
in 2030[a]			
Fuel-powered car	MJ/pkm	0.98	
Electric car	kWh/vkm	0.17	[46]
Bus	MJ/pkm	0.56	
Freight	MJ/tkm	1.51	

[a]assuming linear efficiency improvement from [47].

Table 10: lower heating value (LHV) and exergy of products and fuels[a].

Product	**LHV [MJ/kg]**	**Exergy [MJ/kg]**
FT fuel	44.81	47.94
Methanol	19.83	21.22
DME	28.83	30.84
SNG	47.89	52.12
Hydrogen	119.70	116.50
Pulp	8.15	9.21
Diesel	42.61	NA
Gasoline	43.45	NA
Nat. gas	50.02	NA

[a]LHV based on flowsheeting results, exergy calculated with factors provided in [48].

A.5 Demands of residential district

The average transportation demand is summarized in Table 11, information on the heating and electricity demands of the district, as well as the weather data is provided in Table 12 for average annual data. In Figure 1, samples of the hourly demand profiles included in the model are presented and normalized on the respective annual averages.

Table 11: Shares of passenger vehicles in France for 2019 and 2030.

Value	Unit	Commodity	Reference
		2019	[49]
27	%	Gasoline	
71	%	Diesel	
2	%	Electricity and others	
		2030	[50]
16	%	Gasoline	
24	%	Diesel	
60	%	Electricity and others	

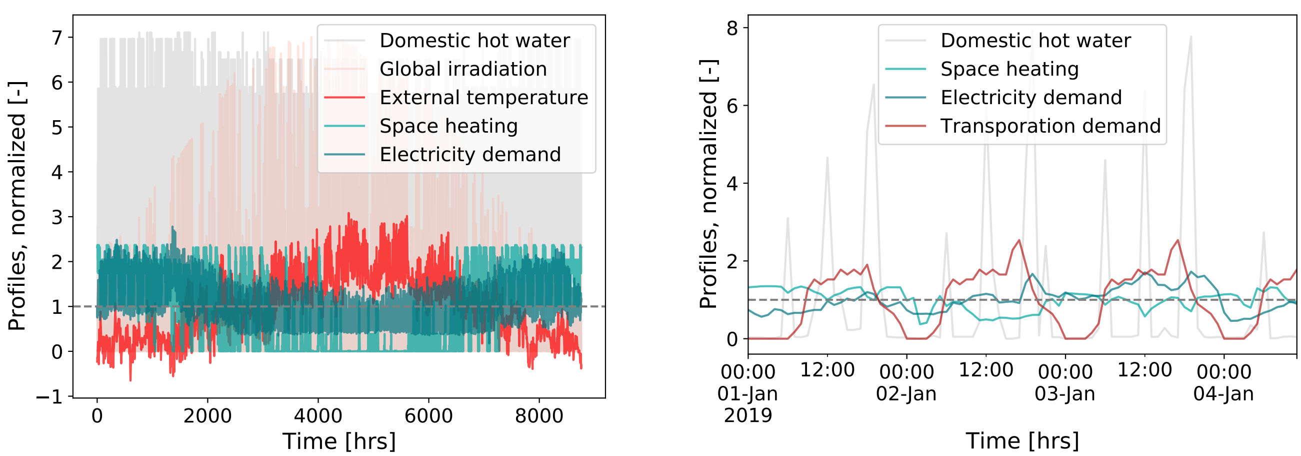

(a) Hourly profile, one year

(b) Hourly profile, four days

Figure 1: Hourly district demands and weather data profiles for one year, adapted from Middelhauve [51], PM Stadler [52] and Cedric Terrier, Luise Middelhauve and François Maréchal [53].

Table 12: District demands and weather data.

	Unit	Value	Reference
Size and demands[a]			[51, 52]
Reference size district	capita	568	
Scaling factor district	-	300/150[b]	
Annual average demands per capita[a]			
Domestic hot water demands	kWh	630	[51, 52]
Space heating demand	kWh	4080	[51, 52]
Electricity demand	kWh	1200	[51, 52]
Personal transport demand	pkm	10800	[53]
Freight transport demand	tkm/yr	4300	[54]
Public transport demand	pkm/yr	4500	[49]
Annual average weather data[a]			[51, 52]
Global irradiation G^{I}	W/m^2	135	
External temperature T^{ext}	°C	10.4	

[a]demands and weather data are given as annual average; in the model, data for hourly resolution is included from the respective references, [b]yields a city size of 170000 and 85000 inhabitants.

B Supplementary information on parameter space and the solution synthesis

B.1 Mathematical formulation and heat exchange characteristics of superstructure optimization problem

The mathematical formulation of the superstructure and optimization in the lower level is adapted from [55, 56], it has also been applied and described in detail in previous studies, such as [1, 57]. The main aspects are summarized hereafter; for more details, the interested reader may consult the cited references. For each unit u in the system, energy and mass flow models are built to describe the conversion in the unit regarding streams, physical properties, mass, and energy balances, and to obtain the characteristics of the interfaces offered for integration with other units. Presuming a set of possible units $\mathbf{U}$ and a set of possible system states $\mathbf{T}$, binary decision variables y_u^{use} and $y_{u,t}^{\text{use}}$ define whether a unit is installed and whether it is used in timestep t. Continuous decision variables f_u^{mult} and $f_{u,t}^{\text{mult}}$ describe the size of the installed unit and the level of usage at which it is operated in each period t. Continuous variables f_u^{mult} are constrained by parameterized upper and lower bounds $F_u^{\text{min/max}}$. Similarly, the binary decision variables y_u^{use} and $y_{u,t}^{\text{use}}$ are limited by Y_u that determines whether a unit is considered for the generation of results.

In the superstructure model, these variables are related to each other by the set of Equations 1- 3.

$$F_u^{\min} \cdot y_u^{\text{use}} \leq \quad f_u^{\text{mult}} \leq F_u^{\max} \cdot y_u^{\text{use}} \quad \forall\, u \in \mathbf{U} \tag{1}$$

$$F_u^{\min} \cdot y_{u,t}^{\text{use}} \leq \quad f_{u,t}^{\text{mult}} \leq F_u^{\max} \cdot y_{u,t}^{\text{use}} \quad \forall\, u \in \mathbf{U}, t \in \mathbf{T} \tag{2}$$

$$Y_u \geq \quad y_u^{\text{use}} \geq y_{u,t}^{\text{use}} \quad \forall\, u \in \mathbf{U}, t \in \mathbf{T} \tag{3}$$

Requirements for each resource are satisfied by internal production and imports (Equation 4). The overall resource balance ensures that import, export, production, and consumption are balanced in the system, as formulated in Equation 5. $\dot{m}^{+}_{re,u,t}$ and $\dot{m}^{-}_{re,u,t}$ define the reference mass flow rate of resource re consumed (+) and provided (-), respectively, in unit u at timestep t. For each unit, the mass balance of streams entering and leaving in a timestep t needs to be closed (Equation 6). It needs to be noted that for clarity of the following mass balance formulation, both in and outgoing streams are labeled as resource, with the respective sign (+/-) indicating the direction. In the main text of this thesis, outgoing resources might be referred to as services (se) provided by the mill. More detailed information on the mathematical formulation of the superstructure optimization problem applied in this thesis is provided in [56].

$$\sum_u f_{u,t}^{\text{mult}} \cdot \dot{m}^{-}_{re,u,t} + \dot{M}^{-}_{re,t} - \sum_u f_{u,t}^{\text{mult}} \cdot \dot{m}^{+}_{re,u,t} \geq \quad 0,\ \forall re \in \mathbf{RE}, \forall t \in \mathbf{T} \tag{4}$$

$$\sum_u f_{u,t}^{\text{mult}} \cdot \dot{m}^{+}_{re,u,t} + \dot{M}^{+}_{re,t} - \dot{M}^{-}_{re,t} - \sum_u f_{u,t}^{\text{mult}} \cdot \dot{m}^{-}_{re,u,t} = \quad 0,\ \forall re \in \mathbf{RE}, \forall t \in \mathbf{T} \tag{5}$$

$$\sum_{re} f_{u,t}^{\text{mult}} \cdot (\dot{m}^{+}_{re,u,t} - \dot{m}^{-}_{re,u,t}) = \quad 0,\ \forall u \in \mathbf{U}, \forall t \in \mathbf{T} \tag{6}$$

All units are connected to a utility system, enabling the energy demand and supply profile of each unit to be satisfied, considering their respective temperature-enthalpy profiles. Minimum energy requirements are calculated applying the Pinch analysis and heat recovery approach presented by Marechal and Kalitventzeff [58], based on the work of Linnhoff and Hindmarsh [59]. The list of all stream inlet and outlet temperatures is extracted and ordered to generate the set of temperature intervals $\mathbf{K}$ of the size N^k [56]. The energy balance is closed in each temperature interval k (Equation 7), and residual heat ($\dot{R}_{t,k}$) flows from higher to lower temperature levels. Following thermodynamic feasibility, cascaded heat flows are positive, while values in both the first and the last interval are zero (Equation 8). $\dot{q}_{u,t,k}$ represents the reference heat load for unit u in timestep t and temperature interval k [55].

$$\forall k \in \mathbf{K}$$

$$\sum_u \dot{q}_{u,t,k} \cdot f_{u,t}^{\text{mult}} + \dot{R}_{t,k+1} - \dot{R}_{t,k} = 0 \quad \forall t \in \mathbf{T} \tag{7}$$

$$\dot{R}_{t,k} \geq 0, \quad \dot{R}_{t,1} = \dot{R}_{t,N^k+1} = 0 \quad \forall t \in \mathbf{T} \tag{8}$$

In this work, the described mixed integer linear programming (MILP) formulation is further enhanced by simultaneous optimization of water and energy developed by Kermani et al. [60], where the thermal characteristics of water streams are considered for heat integration.

Within the mathematical formulation of the optimization problem in the lower-level framework, the energy and process models relevant to the superstructure are organized in so-called clusters. Clusters are defined as entities that can exchange resources freely among each other, but heat can only be exchanged between the different clusters by means of hot water loops or evaporation and condensation of water in the steam network [2]. Thus, per cluster, the heat cascade is defined, as described in Section B.1. Table 13 displays the organization of process units in different clusters for the analyzed system of combined pulp and fuel production, adapted from [2] and enhanced for considering fuel production.

Table 13: Cluster structure in lower-level optimization problem and included process units.

Cluster digester	**Cluster recovery boiler**	**Cluster fuel production**
Washing	Evaporator	Methanol synthesis
Digester	Recovery boiler	DME synthesis
Recausticizer	Biomass boiler	SNG production
		FT fuel synthesis
		Hydrothermal gasification
		Electrolysis
Cluster pulp machine		
Pulp machine		
Bleaching		

B.2 Complexity reduction by means of time series aggregation

Time series aggregation (TSA) methods have gained remarkable significance in the modeling and design of a wide range of energy system applications where seasonal, daily, or hourly variations in demand, supply, or parameter spaces are of importance. A comprehensive review is provided by Hoffmann et al.

[61], investigating TSA methods for modeling energy systems. Schütz et al. [62] compare aggregation methods based on their performance; it was found that k-medoids is most reliable when approximating costs of systems by means of TSA, which is also confirmed by Hoffmann et al. [61].

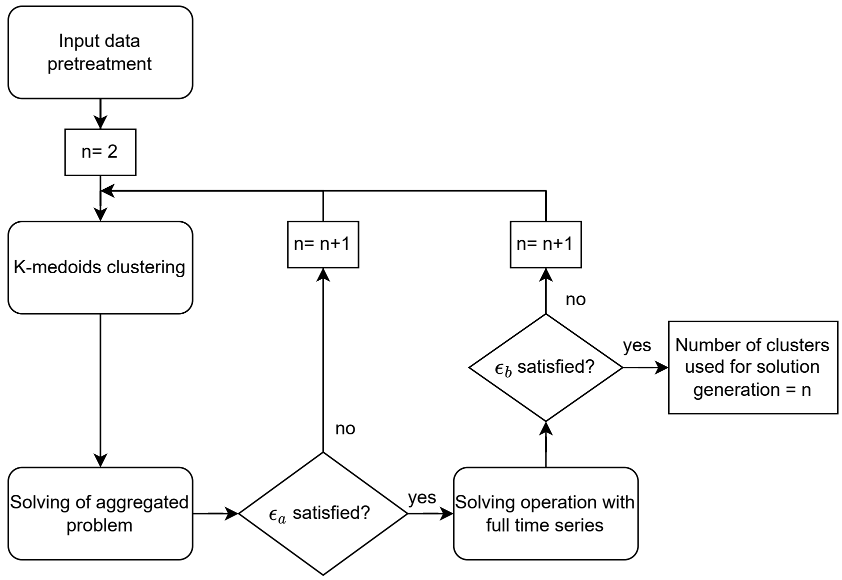

Figure 2: Proposed algorithm for determining the required number of clusters, adapted from Middelhauve et al. [63], Baumgärtner et al. [64] and Bahl et al. [65].

For determining the required number of clusters for analyzing the above-described superstructure adequately, a systematic method for bounding the error of the aggregation in the objective function is followed, as proposed by Baumgärtner et al. [64] and Bahl et al. [65] and further developed by Middelhauve et al. [63]. In each iteration of the incremental increase of TSA resolution, an upper and lower bound of the objectives are evaluated until a convergence criterion on the gap is met. The lower bound is derived from solving the relaxed problem, whereas the upper bound is defined as the solution of the operating problem in consideration of the complete time series and fixed unit sizes given by the relaxed solution [63–65]. Another convergence criterion is considered, in which the relaxed solution of a proposed number of clusters n is compared to the previous solution for $n-1$ clusters. Only when a defined convergence criterion is reached, the operating problem is evaluated for the full-time series, fixing the unit decisions to the findings of the relaxed solution. The procedure for TSA is displayed in Figure 2.

B.3 Parameter sampling and time-dependency

For the consumed resources $re \in RE$ and provided services $se \in SE$, the nominal prices displayed in Table 14 are included. Impact factors are taken from the Ecoinvent database, version 3.6 [66]. As mentioned in the main article, samples are drawn twice from the parameter space, once for solution generation and once during solution exploration. For sampling when generating and exploring solutions, latin hypercube sampling (LHS) is applied for all parameters that are not assumed to be time-dependent. Table 15 gives an overview of the parameter variations considered in both sampling steps, not including time-dependent parameters such as electricity and fuel prices as well as the impact factors of electricity.

Table 14: Nominal values of key economic parameters considered in solution generation and exploration.

Parameters	**Unit**	**Value**	**Reference**
Interest rate	%	6	
Expected lifetime	years	20	
Wood price	USD/kg	0.093	[67]
Pulp price	USD/kg.	0.882	[68]
Electricity price[a]	USD kWh	0.105	[69]
Natural gas price	USD/kWh	0.026	[70]
FT price	USD/kg	-1.108	[71]
Methanol price	USD/kg	-0.390	[72]
DME price	USD/kg	-0.470	[73]
SNG price	USD/kWh	-0.075	[74]
H_2 price	USD/kg	-2.500	[75]
Quicklime price	USD/kg	0.117	[76]
Freshwater price	USD/kg	0.0012	[77]
Landfill price	USD/kg	0.0013	[78]
CO_2 sequestration: transport	USD/kg/250 km	4	[79]
CO_2 sequestration: storage	USD/kg	11	[80]
Waste heat to district heating	USD/kWh	0.075	[81]
Diesel price[b]	USD/l	1.439	[82]
Gasoline price[b]	USD/l	1.515	[82]
Residential heating mix[c]	USD/kWh	0.0689	[36]

[a]annual mean, variation with electricity price from [83], [b]annual mean, variation from WTI crude oil price from [84], [c]current energy mix for heating and cost adapted from [36].

For the time-dependency of energy commodities, the historical behavior of natural gas, electricity, and crude oil is considered. In the superstructure model, it is assumed that SNG prices follow trends of natural gas, whereas prices of liquid fuels follow the crude oil prices [86]. Annual means and the references for time-dependent economic data are provided in Table 14.

For including the time-dependent variation in the superstructure model for solution generation, the available historical, time-dependent data is varied by two parameters: one that shifts the observed data either up or down and one that adds noise to the observed data points. The noise added follows a normal distribution with the standard deviation equaling half of the observed standard deviation in the historical

Table 15: Sampling characteristics of parameter space.

Parameter	Description	Variation[a]
$p^{\mathrm{un}}(u)$	Normalized variation of investment cost of unit $u \in U^*$, U^* = hydrolysis, salt separator, hydrothermal gasification, sulfur removal, CO_2 removal	± 50
$p^{\mathrm{un}}(u)$	Normalized variation of investment cost of unit $u \in U$, U = electrolysis, co-electrolysis, brine electrolysis, dry biomass pretreatment, gasification, gas conditioning, fuel synthesis reactors (FT, MeOH, DME), SNG synthesis, storage tanks, PV, DHN, mineralization	± 20 [85]
$i^{\mathrm{un}}(r)$	Normalized variation of impact of resource $r \in r$, except for electricity	± 20
$r^{\mathrm{un}}(r)$	Normalized variation of market price of resource $r \in r$, except for electricity, natural gas, SNG and biofuels[b]	± 20

[a]all parameters sampled with Latin Hypercube Sampling during solution generation and uniformly distributed for solution exploration. Parameters for which time-dependency is acknowledged are not displayed, [b]SNG, natural gas are considered to follow natural gas trends, biofuels are considered to follow crude oil prices.

data. The newly-obtained data is clustered based on the required number of clusters determined by TSA and used as input for each formulated problem solved by the lower-level framework.

To ensure realistic data points are used for result generation, a literature review on correlations between electricity, crude oil, and natural gas prices is conducted. Historically, natural gas and refined petroleum products have been used as close substitutes in power generation and industry, leading to natural gas prices tracking the prices of crude oil [87]. A strategic statistical analysis of the integrated energy market in Europe is addressed by Bencivenga, Sargenti and D'Ecclesia [87], investigating the short-run relationship between oil, natural gas, and electricity in the European energy markets, and identifying possible long-run equilibrium relationships. Correlation analysis presented itself as non-effective due to the non-stationarity of the data, but cointegration was able to detect a relationship between the individual commodities [87]. In 2014, a report requested by the European Parliament was released, investigating the dependencies in the European energy market [88]. Electricity prices tend to vary considerably throughout Europe and generally show a moderate correlation to oil price developments. Different Merit-order curves in different countries lead to different electricity prices, and market integration into a single electricity market in Europe has not yet been fully achieved [88]. Generally, oil product prices such as diesel and gasoline are strongly related to crude oil prices because of the high share of feed-stock costs in their production [88]. The main pathway of high oil prices being translated into gas and electricity prices was originally induced by the still dominant practice of indexing gas prices to oil prices, prevalent in most gas supply contracts in Europe. It was found that even though gas and oil suppliers share common fundamental price drivers, if oil indexation is absent, gas and oil prices are often decoupled [88]. Recently, an increasing share of studies has addressed the inter-dependencies of actors in the energy market, especially encouraged by the increasing price volatility in the energy commodity markets, addressing risk management in the financial sector and the increasing interest in clean energy technology [89–91].

To acknowledge both time-dependent price and impact variation and inter-dependencies between commodity prices in this study, the covariance of electricity prices regarding oil, natural gas prices, and environmental impact are calculated for different temporal resolutions. Between the electricity price and the impact, a positive correlation can be observed, meaning that more expensive electricity can be associated with a higher impact. For the oil and natural gas prices, no strong correlation is observed, even though both are mainly driven by the same components [86]. Reasons for this might be the different time-resolution of the obtained data, as well as the much more dynamic character of the electricity price that makes observations on correlation on an hourly basis challenging. Daily and biannual data reveal higher correlations, but since the data set used in this study is supposed to represent typical hours, this information is not adequate to draw conclusions.

Therefore, a ratio-based approach is applied instead of relying on the covariance, where oil and natural gas prices are sampled as previously described. A sample is accepted if the ratios between electricity price, gas price, and oil price are within the observed proportions in the historical data set. Obtained samples are then used to scale the energy prices included in the superstructure model. The price for SNG and natural gas is scaled with the sampled data for natural gas, liquid fuel prices with the crude oil price, and electricity prices with the electricity price sample. The applied ratios for acceptance are displayed in Table 16.

Table 16: Accepted ratios for sampling commodity prices, based on historical normalized prices.

Ratios [%]	**Electricity price**	**Oil price**	**Natural gas price**
Electricity price	1	40-800	90-120
Oil price	-	1	60-115
Natural gas price	-	-	1

B.4 Country-specific data

Country-specific data used to extrapolate the analysis to the European level is provided in Table 17.

Table 17: Country-level data to scale results to European level[a].

Country	M^{pulp-}	$c^{nat.gas}$	$c^{gasoline}$	c^{diesel}	c^{elec} [2019]	ei^{elec} [2019]	$c^{elec,*,b}$	$ei^{elec,*,b}$	$Inh.^{country}$	$Emi^{country}$
Unit	kt	EUR/kWh	EUR/l	EUR/l	EUR/kWh	g CO_{2-eq}/kWh	EUR/kWh	g CO_{2-eq}/kWh	Mio. capita	Mio t CO_{2-eq}
Reference	[92]	[70]	[82]	[82]	[69]	[83]	[93]	[93]	[94]	[95]
Belgium	1025	0.02	1.41	1.32	0.08	214.17	0.28	152.16	11.56	106.43
Bulgaria	242	0.03	1.09	1.11	0.09	281.40	0.15	40.94	6.92	49.19
Czechia	557	0.03	1.24	1.24	0.07	763.99	0.19	55.66	10.72	113.34
Germany	2326	0.03	1.43	1.27	0.08	431.31	0.18	54.86	83.20	728.74
Estonia	222	0.03	1.33	1.32	0.08	561.79	0.18	40.24	1.33	11.56
Spain	1456	0.03	1.29	1.22	0.09	224.69	0.14	37.48	47.37	274.74
France	1626	0.03	1.50	1.44	0.08	69.10	0.15	37.19	68.10	392.96
Croatia	47	0.03	1.34	1.32	0.09	346.72	0.13	34.91	4.04	23.76
Italy	334	0.03	1.57	1.48	0.09	383.81	0.13	34.91	59.33	381.25
Hungary	28	0.03	1.17	1.23	0.09	375.98	0.24	61.02	9.74	62.82
Netherlands	34	0.02	1.65	1.36	0.07	530.93	0.21	52.74	17.50	164.33
Austria	2090	0.03	1.24	1.21	0.08	251.44	0.15	27.92	8.93	73.60
Poland	1623	0.03	1.16	1.17	0.07	209.93	0.17	43.33	38.31	376.04
Portugal	2745	0.03	1.49	1.36	0.09	295.27	0.14	35.48	10.31	57.56
Slovenia	92	0.03	1.29	1.25	0.08	342.80	0.25	84.81	2.11	15.85
Slovakia	653	0.03	1.33	1.23	0.09	399.04	0.11	27.6	5.46	37.05
Finland	11 600	0.04	1.52	1.41	0.06	182.71	0.14	34.49	5.53	47.78
Sweden	12 079	0.03	1.48	1.51	0.07	37.29	0.07	45.98	10.38	46.28
Norway	983	0.02	1.52	1.42	0.07	63.52	0.11	40.24	5.39	49.27
Switzerland	92	0.08	1.60	1.74	0.07	178.25	0.20	82.01	8.77	43.41
European Union (EU)	N/A	0.03	1.45	1.36	0.08	337.00	0.16	47.54	448.26	3298.24

[a]for fossil fuels, non-country specific environmental impacts (EIs) are assumed, taking cradle-to-gate emission data from Ecoinvent [66] for IPCC 2013, global warming potential (GWP) 100a, and direct emissions from burning fuels into account: $ei^{diesel} = 0.340$ kg CO_{2-eq}/kg, $ei^{gasoline} = 0.309$ kg CO_{2-eq}/kg, $ei^{nat.gas} = 0.277$ kg CO_{2-eq}/kg, $ei^{H_2} = 2.535$ kg CO_{2-eq}/kg, [b]"*" refers to a future, defossilized electrical grid, with characteristics adapted from Santecchia [93].

C Supplementary information on the results

Choice of residential district size

For determining an adequate size of the district to be considered for integration, the performance of conventional mill operation is analyzed with different district sizes, allowing for no conventional heating of the district. The sensitivity analysis reveals that for the assumed heating demands (Table 8), a city size of 170000 inhabitants could theoretically be heated by the mill, given the mill is operating in a conventional mode without fuel production and other additional process units. For the presented study, a district size of 85000 is chosen, to allow for the analysis of trade-offs between the provision of different energy commodities. However, it needs to be noted that the outcomes of the study, specifically the reported expenses or emission reduction potentials per inhabitant, are largely linked to the assumption of district size.

System configurations

The results of optimization for Perspective S with a district size of 85000 inhabitants is presented in Table 18. The configurations that are selected by the internal optimization and manually are highlighted in grey.

D Design references

Icons for describing the superstructure development were extracted from Flaticon: www.flaticon.com.

Glossary

CFB circulating fluidized bed.

DHN district heating network.

DME dimethyl ether.

EI environmental impact.

ENF entrained flow.

EU European Union.

Table 18: Results of system analysis with district size of 85000 capita.

ID	$\eta^{self,electricity}$	$\eta^{self,transport}$	$\eta^{self,heating}$	$\eta^{self,combined}$	S1	S12	$c^{avoidance}$	ΔEI/cap	ΔTOTEX/cap
	%	%	%	%	%	%	USD/t CO_2	kg CO_2	USD
0	41.3	60.1	46.3	51.3	46.4	328.3	9.3	654.4	6.1
1	44.8	9.8	46.9	36.0	18.5	394.9	-52.9	787.3	-41.7
2	44.3	11.1	47.0	36.3	18.7	343.4	-106.2	684.6	-72.7
3	43.3	56.9	44.5	49.5	47.3	300.1	-88.0	598.3	-52.6
4	42.6	69.7	44.0	52.9	51.3	318.1	-84.6	634.2	-53.7
5	44.1	91.1	40.7	57.8	59.1	404.2	25.5	805.8	20.5
6	43.0	58.3	44.4	49.8	47.6	355.2	-81.3	708.0	-57.5
7	42.5	69.4	44.0	52.8	51.2	347.1	-71.7	692.0	-49.6
8	42.4	67.4	44.3	52.4	50.5	289.4	-136.5	576.9	-78.7
9	44.7	50.4	44.0	47.7	45.6	408.6	5.1	814.6	4.1
10	44.8	7.0	46.5	35.0	17.1	444.7	-61.6	886.5	-54.6
11	44.7	9.2	46.7	35.7	18.1	369.0	-68.3	735.7	-50.2
12	44.6	7.0	50.8	37.3	16.7	469.8	-6.2	936.6	-5.8
13	53.8	3.7	40.1	33.7	21.8	496.3	230.4	989.5	227.9
14	82.2	0.2	26.5	29.3	39.1	550.0	920.2	1096.4	1008.9
15	43.5	100.0	40.9	60.5	62.3	434.9	52.6	867.0	45.6
16	43.5	100.0	41.8	60.8	62.7	441.0	72.0	879.2	63.3
17	52.7	100.0	36.9	57.2	69.7	469.0	328.0	935.0	306.7
18	50.5	100.0	38.1	57.9	67.8	464.7	275.9	926.4	255.6
19	82.2	100.0	24.8	47.2	89.3	525.5	1014.7	1047.5	1062.9
20	82.2	100.0	24.8	47.2	89.3	525.5	1024.7	1047.6	1073.5

Table 19: Author acknowledgments of icons from Flaticon.

Icons	Author's website hyperlink
Solar panel icon, electric pole icon, worker icon, boiler icon, paper stack icon, tree icon	Freepik
Bus icon	Hight Quality Icons
Car icon	fjstudio
Electric car icon, truck icon	kosonicon
House icon	Kiranshastry
Building icon, power generation icon	Smashicons
Fuel icon	Those Icons
Factory icon	monkik
People icon	Vitaly Gorbachev
Solar panel icon	Khoirul Huda

FICFB fast internally circulating fluidized bed.

FT Fischer-Tropsch.

GWP global warming potential.

LHS latin hypercube sampling.

LHV lower heating value.

MEA monoethanolamine.

MILP mixed integer linear programming.

SNG synthetic natural gas.

TSA time series aggregation.

WGS water gas shift.

References

[1] J Granacher, TV Nguyen, R Castro-Amoedo, EC McDonald and F Maréchal. "Enhancing biomass utilization by combined pulp and fuel production". In: *Frontiers in Energy Research* 10 (2022).

[2] M Kermani, ID Kantor, AS Wallerand, J Granacher, AV Ensinas and F Maréchal. "A Holistic Methodology for Optimizing Industrial Resource Efficiency". en. In: *Energies* 12.7 (Jan. 2019), p. 1315.

[3] K Pettersson and S Harvey. "Comparison of black liquor gasification with other pulping biorefinery concepts – Systems analysis of economic performance and CO2 emissions". In: *Energy*. 7th Biennial International Workshop "Advances in Energy Studies" 37.1 (Jan. 2012), pp. 136–153.

[4] TN Adams. *Lime kiln principles and operations*. en. Tech. rep. Seattle: Tappi, 2007, p. 15.

[5] DR Sanchez. *Recausticizing - Principles and Practice*. en. Tech. rep. Orlando, FL: Tappi, 2000, p. 30.

[6] AdS Castro and LS Figueiredo. "Optimization of lime kilns based on strategies of advanced process control - case study Cenibra". en. In: *5 th International Colloquium on Eucalyptus Pulp*. Bahia, Brazil, May 2011, p. 10.

[7] J Gullichsen and CJ Fogelholm. *Chemical Pulping, Part 2*. en. Papermaking science and technology. Fapet Oy, 1999.

[8] Per Lundqvist. "Mass and energy balances over the lime kiln in a kraft pulp mill". en. PhD thesis. 2009.

[9] M Gassner, F Vogel, G Heyen and F Maréchal. "Optimal process design for the polygeneration of SNG, power and heat by hydrothermal gasification of waste biomass: Process optimisation for selected substrates". en. In: *Energy & Environmental Science* 4.5 (Apr. 2011), pp. 1742–1758.

[10] JA Onwudili and PT Williams. "Hydrothermal reactions of sodium formate and sodium acetate as model intermediate products of the sodium hydroxide-promoted hydrothermal gasification of biomass". en. In: *Green Chemistry* 12.12 (2010). Number: 12, p. 2214.

[11] M Magdeldin and M Järvinen. "Supercritical water gasification of Kraft black liquor: Process design, analysis, pulp mill integration and economic evaluation". en. In: *Applied Energy* 262 (Mar. 2020), p. 114558.

[12] M Schubert, J Aubert, JB Müller and F Vogel. "Continuous salt precipitation and separation from supercritical water. Part 3: Interesting effects in processing type 2 salt mixtures". en. In: *The Journal of Supercritical Fluids* 61 (Jan. 2012), pp. 44–54.

[13] JS Luterbacher, M Fröling, F Vogel, F Maréchal and JW Tester. "Hydrothermal Gasification of Waste Biomass: Process Design and Life Cycle Asessment". In: *Environmental Science & Technology* 43.5 (Mar. 2009), pp. 1578–1583.

[14] M Magdeldin, T Kohl and M Järvinen. "Process modeling, synthesis and thermodynamic evaluation of hydrogen production from hydrothermal processing of lipid extracted algae integrated with a downstream reformer conceptual plant". en. In: *Biofuels* 7.2 (Mar. 2016). Number: 2, pp. 97–116.

[15] A Mian, AV Ensinas and F Marechal. "Multi-objective optimization of SNG production from microalgae through hydrothermal gasification". en. In: *Computers & Chemical Engineering* 76 (May 2015), pp. 170–183.

[16] K Özdenkçi, C De Blasio, G Sarwar, K Melin, J Koskinen and V Alopaeus. "Techno-economic feasibility of supercritical water gasification of black liquor". en. In: *Energy* 189 (Dec. 2019), p. 116284.

[17] C Cao, L Guo, H Jin, W Cao, Y Jia and X Yao. "System analysis of pulping process coupled with supercritical water gasification of black liquor for combined hydrogen, heat and power production". In: *Energy* 132 (May 2017).

[18] AM Ribeiro, CA Grande, FV Lopes, JM Loureiro and AE Rodrigues. "A parametric study of layered bed PSA for hydrogen purification". en. In: *Chemical Engineering Science* 63.21 (Nov. 2008). Number: 21, pp. 5258–5273.

[19] M Magdeldin, T Kohl, C De Blasio, M Järvinen, S Won Park and R Giudici. "The BioSCWG Project: Understanding the Trade-Offs in the Process and Thermal Design of Hydrogen and Synthetic Natural Gas Production". en. In: *Energies* 9.10 (Oct. 2016). Number: 10, p. 838.

[20] D Chiche and JM Schweitzer. "Investigation of competitive COS and HCN hydrolysis reactions upon an industrial catalyst: Langmuir-Hinshelwood kinetics modeling". en. In: *Applied Catalysis B: Environmental* 205 (May 2017), pp. 189–200.

[21] Markus Lesemann. *RTI and Eastman Chemical Demonstrate Warm-Temperature Syngas Cleanup Technology*. en. Tech. rep. RTI International, 2013, p. 4.

[22] DL Denton, R Gupta, M Lesemann and B Turk. *RTI Warm Syngas Cleanup Technology Demonstration*. en. 2016.

[23] AD Celebi, S Sharma, AV Ensinas and F Maréchal. "Next generation cogeneration system for industry – Combined heat and fuel plant using biomass resources". In: *Chemical Engineering Science* 204 (Aug. 2019), pp. 59–75.

[24] E Peduzzi. "Biomass To Liquids". en. PhD thesis. Switzerland: EPFL, 2015.

[25] M Gassner and F Maréchal. "Thermo-economic process model for thermochemical production of Synthetic Natural Gas (SNG) from lignocellulosic biomass". en. In: *Biomass and Bioenergy* 33.11 (Nov. 2009), pp. 1587–1604.

[26] L Tock, M Gassner and F Maréchal. "Thermochemical production of liquid fuels from biomass: Thermo-economic modeling, process design and process integration analysis". en. In: *Biomass and Bioenergy* 34.12 (2010), pp. 1838–1854.

[27] S Heyne and S Harvey. "Impact of choice of CO2 separation technology on thermo-economic performance of Bio-SNG production processes". en. In: *International Journal of Energy Research* 38.3 (2014), pp. 299–318.

[28] G Matute, J Yusta and L Correas. "Techno-economic modelling of water electrolysers in the range of several MW to provide grid services while generating hydrogen for different applications: A case study in Spain applied to mobility with FCEVs". en. In: *International Journal of Hydrogen Energy* 44.33 (July 2019). Number: 33, pp. 17431–17442.

[29] X Zhang, Y Song, G Wang and X Bao. "Co-electrolysis of CO2 and H2O in high-temperature solid oxide electrolysis cells: Recent advance in cathodes". en. In: *Journal of Energy Chemistry*. CO2 Capture Storage and Utilization 26.5 (Sept. 2017), pp. 839–853.

[30] R Suciu, P Stadler, A Ashouri and F Maréchal. "Towards energy-autonomous cities using CO2 networks and Power to Gas storage". In: *Proceedings of ECOS 2016*. Postoroz, Slovenia, 2016.

[31] H Ostovari, A Sternberg and A Bardow. "Rock 'n' use of CO 2 : carbon footprint of carbon capture and utilization by mineralization". en. In: *Sustainable Energy & Fuels* 4.9 (2020). Publisher: Royal Society of Chemistry, pp. 4482–4496.

[32] AC Spínola, CT Pinheiro, AGM Ferreira and LM Gando-Ferreira. "Mineral carbonation of a pulp and paper industry waste for CO2 sequestration". en. In: *Process Safety and Environmental Protection* 148 (Apr. 2021), pp. 968–979.

[33] R Castro-Amoedo, J Granacher, MA Daher and F Marechal. "On the role of system integration of carbon capture and mineralization in achieving net-negative emissions in industrial sectors". en. In: *Energy & Environmental Science* (July 2023). Publisher: The Royal Society of Chemistry.

[34] J Sipilä, S Teir and R Zevenhoven. *Carbon Dioxide Sequestration by Mineral Carbonation: Literature Review Update 2005–2007*. Tech. rep. Abo Akademi University, Jan. 2008.

[35] European Technology Platform for Zero Emissions in Fossil Fuel Power Plants. *The costs of CO2 transport: post-demonstration CCS in the EU*. en-AU. Tech. rep. Brussels, Belgium, 2011.

[36] RA Suciu. "Fifth generation district energy systems for low carbon cities". eng. PhD thesis. Lausanne: EPFL, 2019.

[37] F Belfiore. "District heating and cooling systems to integrate renewable energy in urban areas". eng. PhD thesis. Lausanne: EPFL, 2021.

[38] V Masatin, E Latõšev and A Volkova. "Evaluation Factor for District Heating Network Heat Loss with Respect to Network Geometry". en. In: *Energy Procedia*. International Scientific Conference "Environmental and Climate Technologies", CONECT 2015 95 (Sept. 2016), pp. 279–285.

[39] S Henchoz, C Weber, F Maréchal and D Favrat. "Performance and profitability perspectives of a CO2 based district energy network in Geneva's City Centre". en. In: *Energy* 85 (June 2015), pp. 221–235.

[40] P Stadler, L Girardin, A Ashouri and F Maréchal. "Contribution of Model Predictive Control in the Integration of Renewable Energy Sources within the Built Environment". In: *Frontiers in Energy Research* 6 (2018).

[41] L Girardin, F Marechal, M Dubuis, N Calame-Darbellay and D Favrat. "EnerGis: A geographical information based system for the evaluation of integrated energy conversion systems in urban areas". en. In: *Energy*. ECOS 2008 35.2 (Feb. 2010), pp. 830–840.

[42] Federal Statistical Office. *Energy sector*. en. 2022.

[43] EK Vakkilainen. "Steam Generation from Biomass, chapter 3: Boiler process". en. In: *Steam Generation from Biomass*. Ed. by EK Vakkilainen. Butterworth-Heinemann, Jan. 2017, pp. 57–86.

[44] A Ashouri. "Simultaneous Design and Control of Energy Systems". en. Accepted: 2017-10-04T08:17:55Z. Doctoral Thesis. ETH Zurich, 2014.

[45] T Elghozi. *How to calculate the indicators for the transport sector*. en. 2021.

[46] L Calearo, M Marinelli and C Ziras. “A review of data sources for electric vehicle integration studies”. en. In: *Renewable and Sustainable Energy Reviews* 151 (Nov. 2021), p. 111518.

[47] International Energy Agency. *Vehicle fuel economy in major markets 2005-2019*. en. Tech. rep. International Energy Agency, 2021.

[48] J Szargut, DR Morris and FR Steward. *Exergy analysis of thermal, chemical, and metallurgical processes*. English. Berlin, Heidelberg: Springer, 1988.

[49] Eurostat. *Road traffic by type of vehicle*. 2022.

[50] International Energy Agency. *Net Zero by 2050 - A Roadmap for the Global Energy Sector*. en. Tech. rep. International Energy Agency, 2021, p. 224.

[51] L Middelhauve. “On the role of districts as renewable energy hubs”. eng. PhD thesis. Lausanne: EPFL, 2022.

[52] PM Stadler. “Model-based sizing of building energy systems with renewable sources”. eng. PhD thesis. Lausanne: EPFL, 2019.

[53] Cedric Terrier, Luise Middelhauve and François Maréchal. “Potential of electric mobility as service to the grid in renewable energy hubs”. In: *Proceedings of ECOS 2022 - The 35th International Conference on Efficiency, Cost, Optimization, Simulation and Environmental Impact of Energy Systems*. Vol. 35. Copenhagen, Denmark, 2022.

[54] Eurostat. *Territorialised road freight transport, by transport coverage – annual data*. 2022.

[55] M Gassner and F Maréchal. “Methodology for the optimal thermo-economic, multi-objective design of thermochemical fuel production from biomass”. In: *Computers & Chemical Engineering*. Selected Papers from the 17th European Symposium on Computer Aided Process Engineering held in Bucharest, Romania, May 2007 33.3 (Mar. 2009), pp. 769–781.

[56] I Kantor, JL Robineau, H Bütün and F Maréchal. “A Mixed-Integer Linear Programming Formulation for Optimizing Multi-Scale Material and Energy Integration”. In: *Frontiers in Energy Research* 8 (2020), p. 49.

[57] R Castro-Amoedo, N Morisod, J Granacher and F Maréchal. “The Role of Biowaste: A Multi-Objective Optimization Platform for Combined Heat, Power and Fuel”. In: *Frontiers in Energy Research* 9 (2021), p. 417.

[58] F Marechal and B Kalitventzeff. "Process integration: Selection of the optimal utility system". In: *Computers & Chemical Engineering*. European Symposium on Computer Aided Process Engineering-8 22 (Mar. 1998), S149–S156.

[59] B Linnhoff and E Hindmarsh. "The pinch design method for heat exchanger networks". In: *Chemical Engineering Science* 38.5 (1983). 00000, pp. 745–763.

[60] M Kermani, Z Perin-Levasseur, M Benali, L Savulescu and F Marechal. "A novel MILP approach for simultaneous optimization of water and energy: Application to a Canadian softwood Kraft pulping mill". en. In: *Computers & Chemical Engineering* 102 (2017), pp. 238–257.

[61] M Hoffmann, L Kotzur, D Stolten and M Robinius. "A Review on Time Series Aggregation Methods for Energy System Models". en. In: *Energies* 13.3 (Jan. 2020). Number: 3 Publisher: Multidisciplinary Digital Publishing Institute, p. 641.

[62] T Schütz, MH Schraven, M Fuchs, P Remmen and D Müller. "Comparison of clustering algorithms for the selection of typical demand days for energy system synthesis". en. In: *Renewable Energy* 129 (Dec. 2018), pp. 570–582.

[63] L Middelhauve, N Ljubic, J Granacher, L Girardin and F Maréchal. "Data reduction for mixed integer linear programming in complex energy systems". In: *Proceedings of ECOS 2021*. 2021.

[64] N Baumgärtner, B Bahl, M Hennen and A Bardow. "RiSES3: Rigorous Synthesis of Energy Supply and Storage Systems via time-series relaxation and aggregation". en. In: *Computers & Chemical Engineering* 127 (Aug. 2019), pp. 127–139.

[65] B Bahl, A Kümpel, H Seele, M Lampe and A Bardow. "Time-series aggregation for synthesis problems by bounding error in the objective function". In: *Energy* 135 (2017), pp. 900–912.

[66] G Wernet, C Bauer, B Steubing, J Reinhard, E Moreno-Ruiz and B Weidema. "The ecoinvent database version 3 (part I): overview and methodology". en. In: *The International Journal of Life Cycle Assessment* 21.9 (Sept. 2016), pp. 1218–1230.

[67] Food and Agriculture Organization of the United Nations. *Forest Products Annual Market Review, 2018-2019*. Tech. rep. ECE/TIM/SP/48. ISBN: 978-92-1-117218-8. United Nations, 2019.

[68] Index Mundi. *Wood Pulp - Monthly Price*. 2022.

[69] Eurostat. *Electricity prices for non-household consumers - bi-annual data*. 2022.

[70] Eurostat. *Gas prices for non-household consumers - bi-annual data*. 2022.

[71] I Landälv, K Maniatis, Evd Heuvel, S Kalligeros and L Waldheim. *Building up the future, cost of biofuel : sub group on advanced biofuels : sustainable transport forum.* en. Brussels, Belgium: Publications Office of the European Union, June 2018.

[72] Methanex. *Methanex Monthly Average Regional Posted Contract Price History*. 2021.

[73] P Zeman, V Hönig, P Procházka and J Mařík. "Dimethyl ether as a renewable fuel for diesel engines". en. In: *Agronomy Research* 15 (2017).

[74] J Gorre, F Ortloff and C van Leeuwen. "Production costs for synthetic methane in 2030 and 2050 of an optimized Power-to-Gas plant with intermediate hydrogen storage". en. In: *Applied Energy* 253 (Nov. 2019), p. 113594.

[75] International Energy Agency. *The Future of Hydrogen*. en-GB. Technology Report. Paris, France: International Energy Agency, June 2019, p. 203.

[76] Index Mundi. *Lime Prices In The United States, By Type*. 2022.

[77] European Association of Public Water Operators. *Water affordability*. Tech. rep. Brussels: European Association of Public Water Operators, 2016.

[78] Valmet. *The modern white liquor plant*. Tech. rep. Valmet, 2017.

[79] International Energy Agency. *Special Report on Carbon Capture Utilisation and Storage: CCUS in clean energy transitions*. en. Tech. rep. International Energy Agency, 2020, p. 174.

[80] WJ Schmelz, G Hochman and KG Miller. "Total cost of carbon capture and storage implemented at a regional scale: northeastern and midwestern United States". In: *Interface Focus* 10.5 (Oct. 2020), p. 20190065.

[81] G Gullberg, F Ericson and M Eck. *The French District Heating Market – Overview, Opportunities and Challenges*. en. Tech. rep. Swedish Energy Agency, 2019, p. 33.

[82] European Commission. *Weekly Oil Bulletin*. en. 2022.

[83] Entsoe. *European association for the cooperation of transmission system operators for electricity*. en-us. 2022.

[84] Macrotrends LLC. *WTI Crude Oil Prices - 10 Year Daily Chart — MacroTrends*. 2023.

[85] GA Buchner, AW Zimmermann, AE Hohgräve and R Schomäcker. "Techno-economic Assessment Framework for the Chemical Industry—Based on Technology Readiness Levels". In: *Industrial & Engineering Chemistry Research* 57.25 (June 2018), pp. 8502–8517.

[86] US Energy Information Administration. *Factors affecting natural gas prices - U.S. Energy Information Administration (EIA)*. 2022.

[87] C Bencivenga, G Sargenti and RL D'Ecclesia. "Energy markets: crucial relationship between prices". en. In: *Mathematical and Statistical Methods for Actuarial Sciences and Finance*. Ed. by M Corazza and C Pizzi. Milano: Springer Milan, 2010, pp. 23–32.

[88] U Albrecht, M Altmann, J Zerhusen, T Rakhsa, P Maio, A Beaudet, P Trucco, C Egenhofer, A Behrens, J Teusch, J Wieczorkiewicz, F Genoese and G Maisonnier. *The impact of the oil price on EU energy prices*. Tech. rep. Policy Department European Parliament, 2014.

[89] T Kanamura. "A model of price correlations between clean energy indices and energy commodities". In: *Journal of Sustainable Finance & Investment* 12.2 (Apr. 2022), pp. 319–359.

[90] MU Rehman. "Dynamic correlation pattern amongst alternative energy market for diversification opportunities". In: *Journal of Economic Structures* 9.1 (Feb. 2020), p. 16.

[91] N Lange. "Correlation in Energy Markets". en. PhD thesis. Frederiksberg: Copenhagen Business School, 2017.

[92] Eurostats. *Pulp, paper and paperboard*. 2022.

[93] A Santecchia. "Enabling renewable Europe through optimal design and operation". eng. PhD thesis. Lausanne: EPFL, 2022.

[94] Eurostat. *Population and employment*. 2023.

[95] European Environment Agency. *EEA greenhouse gases*. en. Dashboard (Tableau). 2022.